

Electrodeposition of Gold Films from a Glycerol Solution on Carbon Paste Electrode and the Effect of Chemical and Electrochemical Parameters of Electrodeposition on the Electrode Performance in Potassium Ferrocyanide Solution

Elter G. Gama and Gildiberto M. Oliveira*

Curso de Química, Universidade Federal de Goiás, Regional Jataí, CP 03, 75800-000 Jataí-GO, Brazil

The gold electrodeposition process from a glycerol solution on a carbon paste electrode (CPE) was investigated by voltammetry and the morphologies of the electrodeposits were analyzed by scanning electron microscopy (SEM). Voltammetric study indicated that AuCl_4^- was reduced to Au^0 and the process was mixed controlled (mass transport and electron transfer), preceded probably by AuCl_4^- decomplexation. Glycerol affected the kinetic of gold electrodeposition in function of the AuCl_4^- concentration. SEM images indicated that the gold electrodeposit covered totally some of the graphite flake by a homogeneous morphology, regardless of the electrodeposition condition. Moreover, using a full factorial planning it was verified that the deposition charge and potential affected the modified CPE performance in a potassium ferrocyanide solution, while HAuCl_4 and glycerol concentrations affected only by interactions with the other factors.

Keywords: gold electrodeposition, carbon paste electrode, glycerol, planning factorial, voltammetry

Introduction

Carbon paste is a composite material obtained by mixing graphite powder and a binder (nujol, parafine, etc.).^{1,2} The carbon paste electrode (CPE) is used in electroanalysis mainly due to the possibility of changing its composition, which can enhance the method sensibility and selectivity.^{1,2} The modified CPE can be made by introducing a desired substance (organic,^{3,4} inorganic,^{5,6} enzyme,^{7,8} etc.) into the carbon past or on its surface. The modification by metals are made mainly by introducing nanoparticles of the metal, dispersed into the binder, produced by an *ex situ* process.⁹⁻¹⁶ By electrodeposition also is possible to modify the CPE, producing nanoparticles or thin films which cover the graphite flake surface.¹⁷⁻²⁹

The modified CPE by metallic electrodeposits (gold,¹⁷⁻²¹ bismuth,^{22,23} palladium,²⁴⁻²⁶ antimony,^{27,28} silver,²⁹ etc.) has been employed at analysis of various analytes, for example: mercury(II) in water;¹⁷ dopamine¹⁸ and morphine¹⁹ in the presence of ascorbic acid and uric acid; morphine in urine;²⁰ methadone in biological fluids;²¹ heavy metals;^{22,27} nitrobenzene;²³ electrooxidation of oxalic acid;²⁴ hydrogen peroxide, dopamine and ascorbic acid;²⁵ electrocatalytic oxidation of formaldehyde;²⁶ indium, thallium and zinc²⁸

and paraquat.²⁹ Although the use of metallic electrodeposit as modifier on the electrodes surfaces has been very studied and some electrochemical parameters (deposition potential and time deposition) of electrodeposition are investigated on the electrode response,^{22,24} the effect of other electrodeposition parameters are not completely described in these papers, that is, it is not investigated which electrodeposition parameters are main factors or if these factors affect the electrode response by interactions.³⁰ In this context, a factorial planning can be used as tool to find the main factors and its interactions.

The electrodeposition process involves the reduction of metal ion from a solution, which deposit morphology and structure can be influenced by the chemical solution composition and electrochemical parameters of electrodeposition.^{31,32} In order to enhance the features of the metal electrodeposit morphologies (brightness, roughness, levelness, grain size, etc.), a substance named as additive can be introduced into the electrodeposition solution.³¹⁻³⁹ Glycerol has been shown good results for nickel,³⁵ lead,³⁶ zinc,³⁷ copper³⁸ and zinc-nickel³⁹ electrodeposition processes.

The modification of the bulk and surface composition of CPE can affect its performance on the voltammetric response, for example, by changing the effective electrode surface area, the inner ohmic resistance and the electron

*e-mail: gil_mdo@hotmail.com, gildiberto_oliveira@ufg.br

transfer rate. The ferri/ferrocyanide redox couple has been chosen to evaluate the performance of CPE because this redox couple has a well known electrochemical behavior, considered as reversible system.⁴⁰⁻⁵⁰ In this reversible system, it is expected to obtain a difference between the anodic and cathodic peak potentials of 60 mV and a ratio of anodic/cathodic peak current equal to 1. In a reversible system, the rate of electron transfer is higher than the mass transport, showing a high exchange current density to the redox couple.⁵¹

In the present work, the effect of the glycerol on gold electrodeposition process on the CPE was studied by voltammetry and the morphology of the electrodeposit were analyzed by scanning electron microscopy (SEM). In addition, using a factorial planning, it was investigated the effect of some chemical and electrochemical parameters of electrodeposition on the modified carbon past electrode features in ferri/ferrocyanide system reversibility.

Experimental

All chemicals were analytical grade. The solutions were prepared with distilled water throughout. The electrochemical experiment was realized in freshly prepared plating solutions containing H₂AuCl₄ (chloroauric acid, Synth) and C₃H₈O₃ (glycerol, Synth) or K₄Fe(CN)₆ (potassium ferrocyanide, Synth). The NaCl (sodium chloride, Proquimicos) were employed as supporting electrolyte.

UV-Vis spectrums were taken with a PerkinElmer UV-Vis Lambda 35 spectrometer.

The carbon paste (CP) was obtained by mixing graphite powder (Synth, diameter < 50 μm) and mineral oil (Isofar) in a mass ratio of 70:30 in an agate mortar until the paste acquired homogeneous consistency. The electrode was made of a polypropylene syringe (1 mL) with an electrical contact of copper wire.

Electrochemical measurements were recorded with an Ivium Compactstat 800 mA Potentiostat/Galvanostat, using an electrochemical cell with three electrodes. As working, counter and reference electrodes, CPE, platinum wire and Ag/AgCl, KCl 1.0 mol L⁻¹ were employed, respectively.

Scanning electron microscopy (SEM) photographs were taken with a JEOL JSM-IT300LV microscopy. The SEM images were obtained in the backscattered electrons (BSE) mode. To avoid SEM microscopy damage, it was removed the mineral oil from the carbon paste. The samples were prepared cutting off a little piece of the CPE and removing the mineral oil off the carbon paste by successive washing in cyclohexane, ammonium solution (1.4 × 10⁻³ mol L⁻¹) and distilled water. After this, the samples were dried at 80 °C for 4 h.

Results and Discussion

Chemical solution of electrodeposition

The electrodeposition of gold was studied from solutions containing H₂AuCl₄, which forms AuCl₄⁻ ions in solution, and glycerol. Glycerol has OH groups that could act as ligand for Au³⁺ ions. To form a complex with Au³⁺, the glycerol needs to dislocate the chloride ion of the metal ion AuCl₄⁻ at a solution that contains NaCl (0.10 mol L⁻¹), which could be reached in solution with high glycerol concentration. Figure 1 shows the UV-Vis spectrum for the aqueous solution containing H₂AuCl₄:glycerol in the ratios of 1:1, 1:10 and 1:100. It can be seen that the features of the UV-Vis spectrums were similar, showing two peaks (at 224 and 310 nm) related to AuCl₄⁻ species. This result indicated that glycerol did not act as ligand for Au³⁺ in these solutions. In this case, it was investigated the effect of glycerol as additive (brighter, smoothing, etc.) on the gold electrodeposition.³¹⁻³⁹

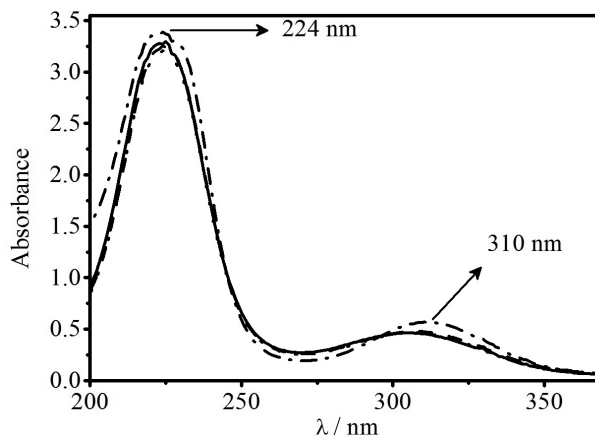


Figure 1. UV-Vis spectrum for aqueous solution containing $1.4 \times 10^{-2} \text{ mol L}^{-1} \text{ NaCl} + 1.4 \times 10^{-4} \text{ mol L}^{-1} \text{ H}_2\text{AuCl}_4$ and glycerol: (—) 0.0 mol L⁻¹; (---) $1.4 \times 10^{-4} \text{ mol L}^{-1}$; (•••) $1.4 \times 10^{-3} \text{ mol L}^{-1}$ and (-•-) $1.4 \times 10^{-2} \text{ mol L}^{-1}$.

Gold electrodeposition process characterization

Electrochemical studies

Figure 2 (dashed curve) shows typical voltammetric curves for the CPE in H₂AuCl₄ solution. It can be seen in the cathodic sweep that the current increased from potential more negative than +0.700 V, showing a peak at +0.600 V (region named c_{AuI}), while in the anodic sweep the current increased at potentials more positive than +0.600 V, showing a peak at +0.900 V (region named a_{AuI}). Reversing the cathodic sweep at +0.45 V (Figure 2 inset), it was observed a crossover at about +0.600 V, indicating Au deposition by a 3D nucleation process.^{33,34,52} This result

indicated that regions c_{Au1} and a_{Au1} probably were related to $AuCl_4^-$ reduction to Au metallic and Au metallic oxidation to $AuCl_4^-$, respectively.

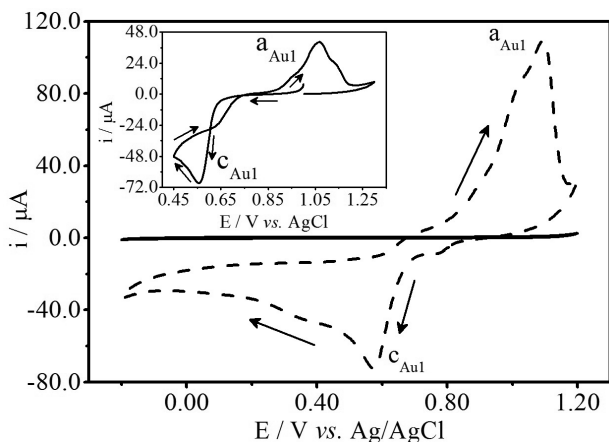


Figure 2. Typical voltammetric curves (3rd cycle at 20 mV s⁻¹) for the CPE in 1.0×10^{-1} mol L⁻¹ NaCl solution containing HAuCl₄: (—) 0.0 mol L⁻¹ and (---) 1.0×10^{-3} mol L⁻¹. Inset: voltammetric curve (1st cycle at 20 mV s⁻¹) with cathodic sweep reversed at +0.45 V. Subscript Au in c_{Au} and a_{Au} indicate solution containing HAuCl₄.

It must be stressed that glycerol could be oxidized,^{32,33} thus the voltammetric studies were performed with the CPE in 1.0×10^{-1} mol L⁻¹ NaCl solution containing various glycerol concentrations (Figure 3a). Figure 3b shows four successive cycles for the voltammetric curves obtained in 1.0×10^{-1} mol L⁻¹ glycerol. The voltammetric sweep begins at +0.800 V in direction to more negative potential, reversing the cathodic sweep at -0.200 V and the anodic sweep at +1.200 V. These voltammetric curves showed two cathodic (c_{gly1} and c_{gly2}) and two anodic (a_{gly1} and a_{gly2}) regions, which peak currents increased with increasing

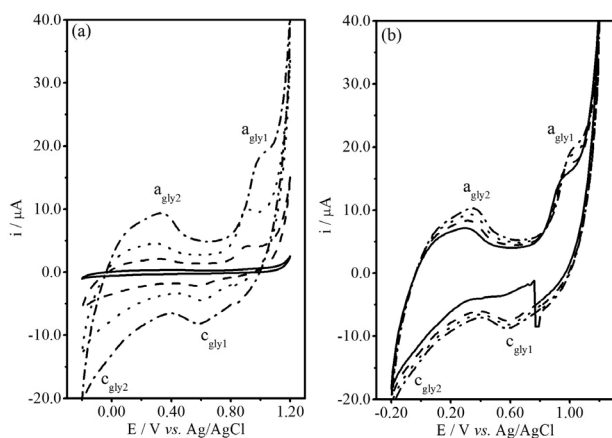


Figure 3. Typical voltammetric curves (at 20 mV s⁻¹) for the CPE in 1.0×10^{-1} mol L⁻¹ NaCl solution containing (a) various glycerol concentrations: (—) 0.0 mol L⁻¹; (---) 1.0×10^{-3} mol L⁻¹; (•••) 1.0×10^{-2} mol L⁻¹ and (-•-) 1.0×10^{-1} mol L⁻¹, 3rd cycle; (b) 1.0×10^{-1} mol L⁻¹ glycerol with four cycle successive: (—) 1st, (---) 2nd, (•••) 3rd and (-•-) 4th. Subscript gly in c_{gly} and a_{gly} indicate solution containing glycerol.

glycerol concentration. Regions c_{gly2} and a_{gly2} probably were due to the hydrogen evolution reaction (HER) and H₂ oxidation, respectively. In addition, it can be seen that the HER at c_{gly2} was depolarized with increasing glycerol concentration. It must be stressed that the cathodic current at +0.600 V (Figure 3b) in the first cycle (solid line, 3.16 μA) corresponded to about 36-42%, calculated without subtracting a baseline (17-19%, subtracting a baseline), of that in the second (dashed line, 7.52 μA), third (dotted line, 8.15 μA) and fourth (dashed-dotted line, 8.72 μA) cycles. This result indicated that cathodic process at c_{gly1} depends on the concentration of something that was not present in the first cycle, that is, the products formed during glycerol oxidation in the region a_{gly1} .^{53,54} This result suggested that glycerol oxidation probably can occur in the anodic sweep in parallel to gold oxidation in solution containing HAuCl₄ and glycerol.

Figures 4a and 4b show the voltammetric curves for the CPE in NaCl/HAuCl₄ solution containing various glycerol concentrations. It was observed an increase of the cathodic peak current (i_{cp}) in function of the glycerol concentration (Figure 4a), showing a peak current at c_{Augly1} of 72.3 μA (solid line, without glycerol), 82.8 μA (dashed line, 1.0×10^{-3} mol L⁻¹ glycerol), 88.2 μA (dotted line, 1.0×10^{-2} mol L⁻¹ glycerol), 90.6 μA (dashed-dotted line, 1.0×10^{-1} mol L⁻¹ glycerol). These peak currents increases more than the observed in solution containing only glycerol (Figure 3a), that showed peak current at c_{gly1} of 2.10 μA (dashed line, 1.0×10^{-3} mol L⁻¹ glycerol), 4.51 μA (dotted line, 1.0×10^{-2} mol L⁻¹ glycerol), 8.05 μA (dashed-dotted line, 1.0×10^{-1} mol L⁻¹ glycerol). In addition, it can be seen in Figure 4b that the i_{cp} values in the first (solid line,

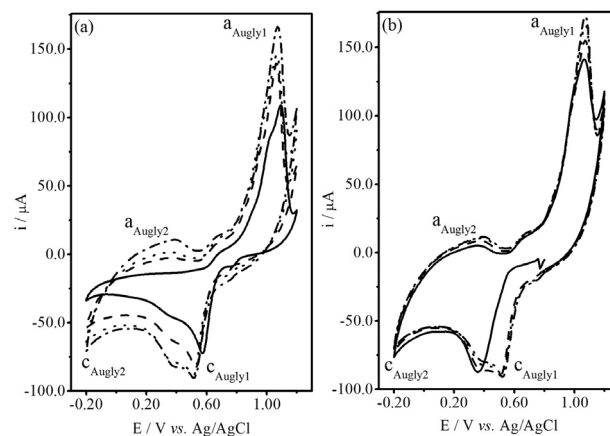


Figure 4. Typical voltammetric curves (at 20 mV s⁻¹) for the CPE in 1.0×10^{-1} mol L⁻¹ NaCl + 1.0×10^{-3} mol L⁻¹ HAuCl₄ solution containing: (a) various glycerol concentrations: (—) 0.0 mol L⁻¹, (---) 1.0×10^{-3} mol L⁻¹, (•••) 1.0×10^{-2} mol L⁻¹ and (-•-) 1.0×10^{-1} mol L⁻¹, 3rd cycle; (b) 1.0×10^{-1} mol L⁻¹ glycerol with four cycle successive: (—) 1st; (---) 2nd; (•••) 3rd and (-•-) 4th. Subscript Augly in c_{Augly} and a_{Augly} indicate solution containing HAuCl₄ and glycerol.

87.1 μA), second (dashed line, 89.4 μA), third (dotted line, 90.6 μA) and fourth (dashed-dotted line, 90.5 μA) cycles were very similar (about 57.9-63.7 μA , obtained subtracting a baseline). This peak current analysis suggested that the i_{cp} increases in Figure 4a were not only due to the reduction of glycerol oxidation products (as discussed in Figure 3a) parallel to AuCl_4^- reduction, but suggested that glycerol affected the kinetic of AuCl_4^- reduction or modified the gold deposit morphologies.

In order to obtain more information about glycerol effects on the gold electrodeposition, a set of voltammetric curves were realized in $\text{NaCl } 1.0 \times 10^{-1} \text{ mol L}^{-1}$ solution containing various HAuCl_4 concentrations, without and with $1.0 \times 10^{-3} \text{ mol L}^{-1}$ glycerol (figure not showed here). Figures 5a and 5b show, respectively, the plots of the cathodic charge (q_c) and the ratio of q_c (solution with/without glycerol) in function of HAuCl_4 concentration. The q_c was measured subtracting a baseline since the cathodic charge could be influenced by the hydrogen evolution reaction (HER) at $c_{\text{Augly}2}$ region, which it was more effective in solution containing glycerol. It can be verified in Figure 5a that q_c increased in function of HAuCl_4 concentration, showing an almost linear (square) and not linear (circle) relation in solution without and with glycerol, respectively. In other hand, the q_c ratio of solution with/without glycerol (Figure 5b) was higher than 1.4, exhibiting a first increase

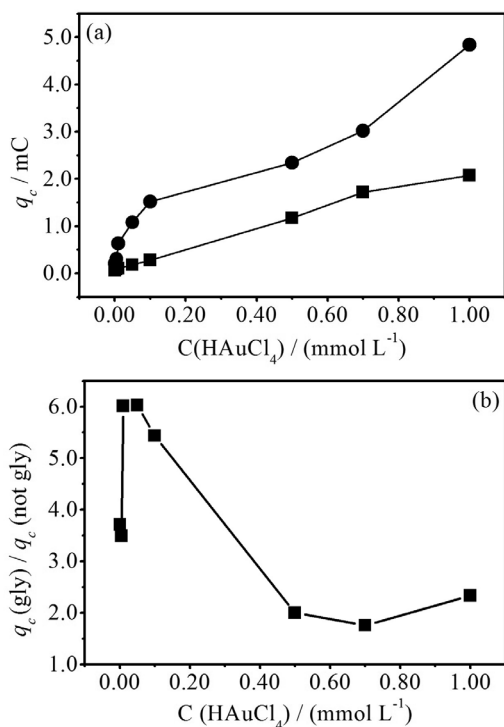


Figure 5. Plot of the (a) q_c ; (b) ratio of q_c (solution with/without glycerol) in function of HAuCl_4 concentration for the voltammetric curves obtained in $1.0 \times 10^{-1} \text{ mol L}^{-1}$ NaCl solution containing various HAuCl_4 concentration, (■) without and (●) with $1.0 \times 10^{-3} \text{ mol L}^{-1}$ glycerol.

(HAuCl_4 concentration up to $1.0 \times 10^{-5} \text{ mol L}^{-1}$), followed by an almost exponential decreases for HAuCl_4 concentration higher than $5.0 \times 10^{-5} \text{ mol L}^{-1}$. This result indicated that the glycerol affected the Au^{3+} kinetic of reduction and depends on HAuCl_4 concentration.

A set of voltammetric curves with various sweep rates (v) were obtained in $1.0 \times 10^{-1} \text{ mol L}^{-1}$ $\text{NaCl}/1.0 \times 10^{-3} \text{ mol L}^{-1}$ HAuCl_4 solution, without and with $1.0 \times 10^{-3} \text{ mol L}^{-1}$ glycerol (figure not shown here). For these voltammetric curves, were verified that: i_{cp} increased with $n^{1/2}$, but not linearly (Figure 6a); cathodic peak potential (E_{cp}) shifted negatively with increasing v (Figure 6b) and $E_{\text{ap}} - E_{\text{cp}}$ decreased with increasing v (Figure 6c). This result suggested that the gold electrodeposition were mixed controlled by mass transport and charge transfer.^{30,33,34,55} Besides, Figure 6d show that $i_{\text{cp}}/n^{1/2}$ decreased in function of v , indicating that a chemical reaction preceding the charge transfer occurred, probably AuCl_4^- decomplexation.^{34,55}

Scanning electron microscopy analysis of the electrodeposits

SEM images were taken to verify the features of the gold electrodeposit morphologies grown on the graphite flakes. It was investigated three electrodeposition parameters: HAuCl_4 concentration (1.0×10^{-6} and $1.0 \times 10^{-4} \text{ mol L}^{-1}$), glycerol added (0 and $1.0 \times 10^{-3} \text{ mol L}^{-1}$) and deposition charge (1.0×10^{-6} and $1.0 \times 10^{-4} \text{ C}$). Figure 7 showed a less magnified SEM image for the graphite powder covered by gold electrodeposits obtained at those conditions. The SEM images were taken at backscattered electrons (BSE) mode, then the white color indicated gold electrodeposits, confirmed by energy-dispersive X-ray spectroscopy (EDS) analysis. This SEM image showed well defined white and black regions, indicating that some graphite flakes were covered and not covered by gold electrodeposit, respectively. It can be supposed that the gold electrodeposition occurred on the graphite flake near the CPE surface/solution interface. The graphite flake not covered by gold is mainly that located into the CPE. Remember that the SEM analysis was made first cutting off a little piece of the CPE, and after, washing this CP to remove the mineral oil.

Figures 8a-d show typical SEM images (10,000 times magnification) of the gold electrodeposits obtained from $1.0 \times 10^{-1} \text{ mol L}^{-1}$ NaCl solution containing two HAuCl_4 concentration (1.0×10^{-6} and $1.0 \times 10^{-4} \text{ mol L}^{-1}$) at two deposition charges (1.0×10^{-6} and $1.0 \times 10^{-4} \text{ C}$). It can be seen that the gold electrodeposit covered totally the graphite flake by a homogeneous morphology, regardless of the HAuCl_4 concentration and the deposition charge. Similar results were obtained for the gold electrodeposits obtained in glycerol solutions (Figures 9a-d). In addition,

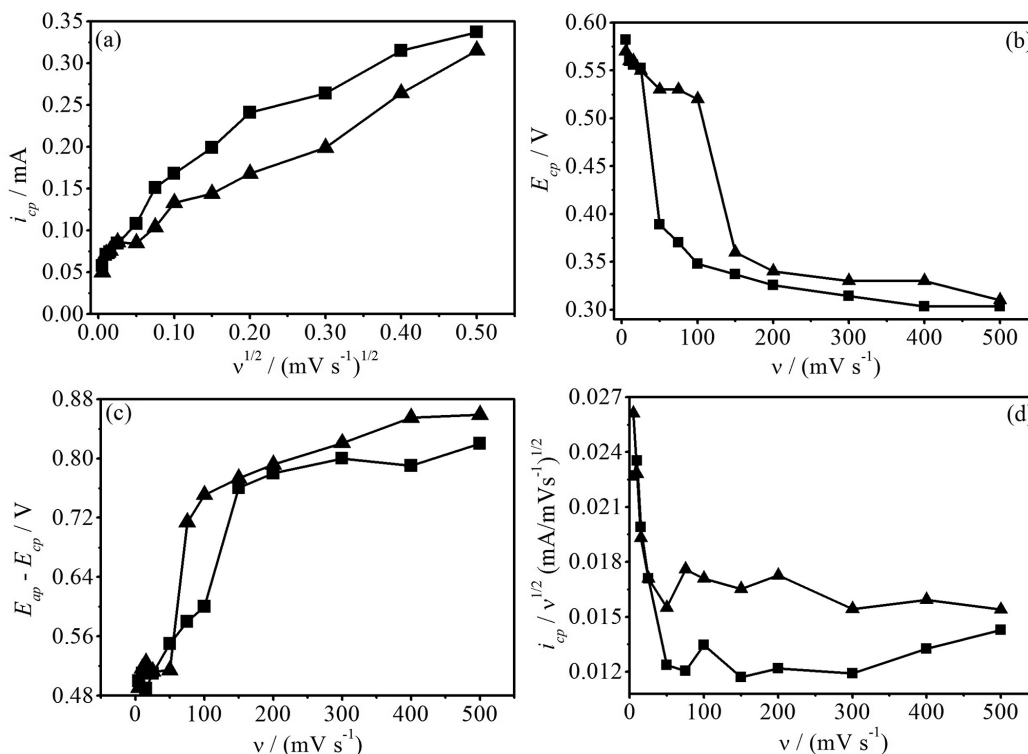


Figure 6. Plots of (a) i_{cp} in function of $n^{1/2}$; (b) E_{cp} ; (c) $E_{ap} - E_{cp}$; (d) $i_{cp}/n^{1/2}$ in function of v for the voltammetric curves obtained in 1.0×10^{-1} mol L⁻¹ NaCl/ 1.0×10^{-3} mol L⁻¹ HAuCl₄ solution, (■) without and (▲) with 1.0×10^{-3} mol L⁻¹ glycerol.

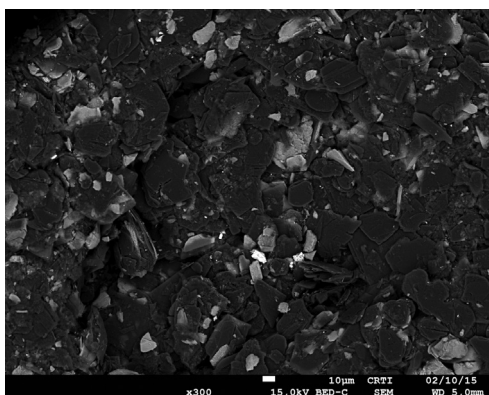


Figure 7. Typical SEM micrograph image of the gold electrodeposits on the CPE obtained potentiostatically at +0.200 V.

from SEM images were observed graphite flakes with diameter smaller than about 50 micrometer, and the thickness was estimated about less than 1 micrometer. As can be seen in Figure 8c, the thickness of the graphite flake covered by gold electrodeposit does not seem to be greater than 1 micrometer. Thus, it can be supposed that the gold electrodeposit was not very thick.

It must be stressed that the SEM analyses were very important to show that the gold electrodeposit covered some graphite flakes with a smoothing deposit, regardless of the chemical and electrochemical condition of electrodeposition. However, despite these similar morphological feature, the CPE performance in ferrocyanide

solution was dependent on the electrochemical deposition condition (conclusion obtained from the factorial design, discussed in Tables 1 and 2).

Gold electrodeposit as modifier on the CPE

In light of the chemical and electrochemical parameters of electrodeposition could affect the gold electrodeposit features and then probably its performance as modifier in the CPE, a voltammetric study was realized in a potassium ferrocyanide solution, analyzing the reversibility of the ferro/ferricyanide system.⁴⁰⁻⁵⁰ In this study was applied a full factorial planning (Table 1) containing two levels for each factors: HAuCl₄ concentration, glycerol added, deposition potential and deposition charge. The response analyzed was the ratio of cathodic-anodic peak current (i_{pa}/i_{pc}) and the difference of cathodic-anodic peak potential (ΔE) for the voltammetric curves obtained at 20 mV s⁻¹.

Figure 10 shows two voltammetric curves obtained in potassium ferrocyanide solution for the CPE not covered and covered by gold electrodeposit obtained from: HAuCl₄ 1.0×10^{-6} mol L⁻¹, glycerol 1.0×10^{-3} mol L⁻¹, at +0.200 V and with 1.0×10^{-4} C (experiment 15, in Table 1). It can be verified in this case that the gold electrodeposit enhance the ferro/ferricyanide reversibility system, decreasing ΔE (from 0.150 to 0.070 V) and i_{pa}/i_{pc} (from

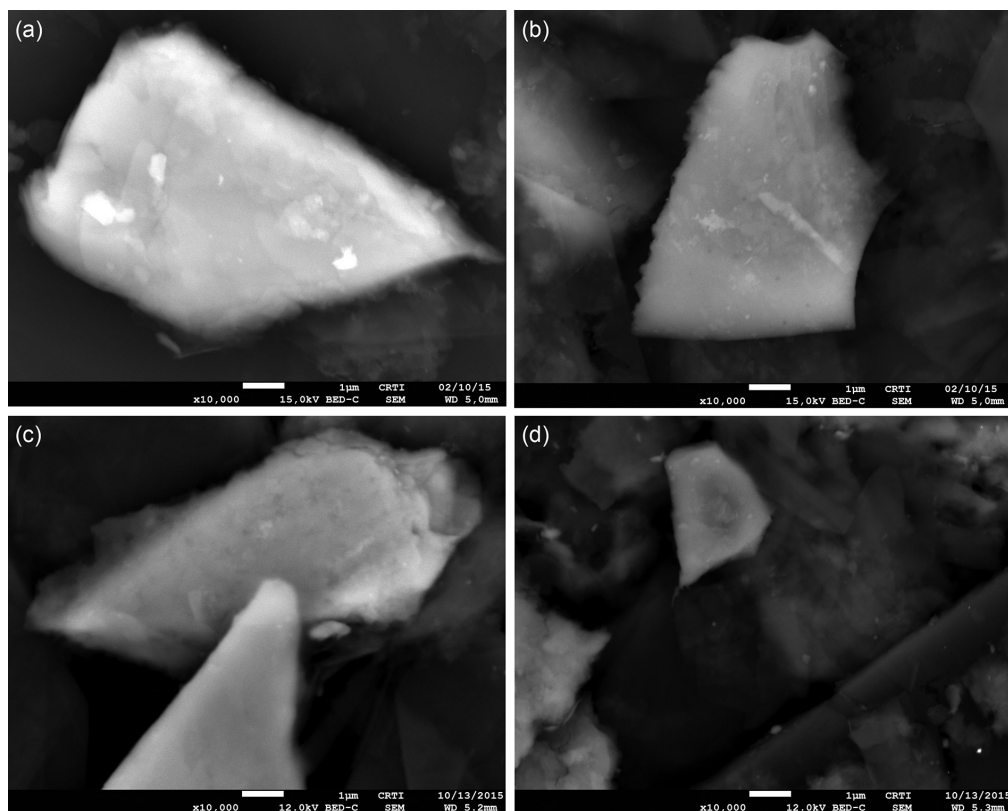


Figure 8. SEM micrographs of the gold electrodeposits on the CPE obtained potentiostatically at +0.200 V from $1.0 \times 10^{-1} \text{ mol L}^{-1}$ NaCl solution containing: (a)-(b) $1.0 \times 10^{-6} \text{ mol L}^{-1}$ HAuCl₄ and (c)-(d) $1.0 \times 10^{-4} \text{ mol L}^{-1}$ HAuCl₄ with (a), (c) $1.0 \times 10^{-6} \text{ C}$ and (b), (d) $1.0 \times 10^{-4} \text{ C}$.

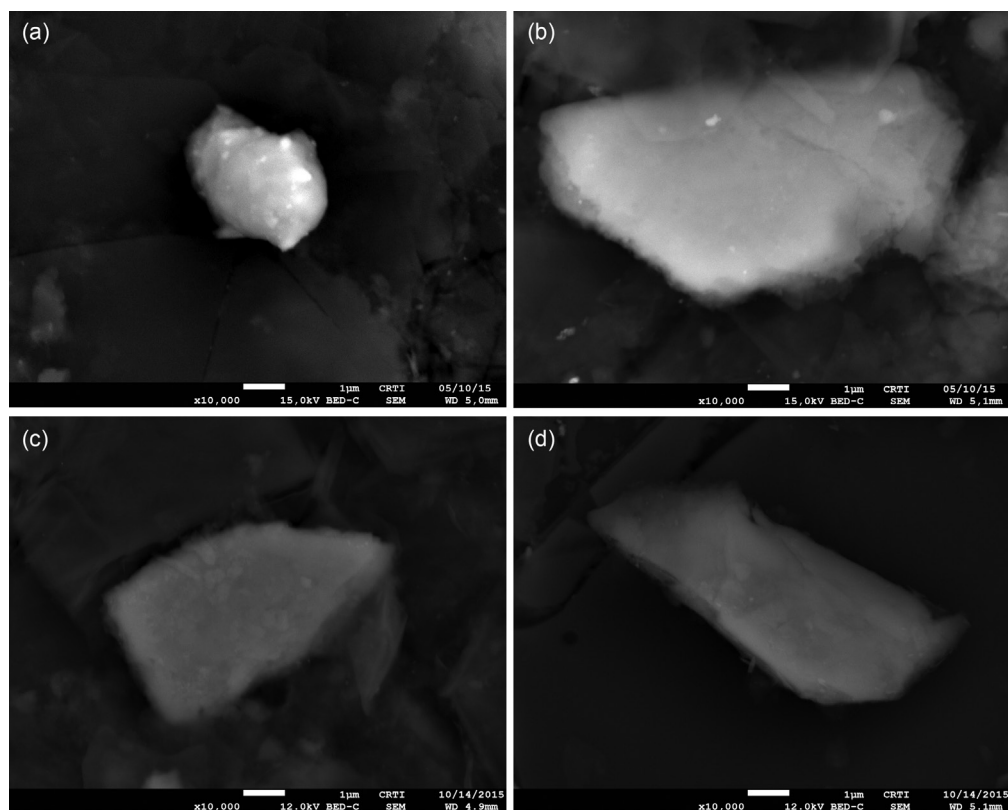


Figure 9. SEM micrographs of the gold electrodeposits on the CPE obtained potentiostatically at +0.200 V from $1.0 \times 10^{-1} \text{ mol L}^{-1}$ NaCl/ $1.0 \times 10^{-3} \text{ mol L}^{-1}$ glycerol solution containing: (a)-(b) $1.0 \times 10^{-6} \text{ mol L}^{-1}$ HAuCl₄ and (c)-(d) $1.0 \times 10^{-4} \text{ mol L}^{-1}$ HAuCl₄ with (a), (c) $1.0 \times 10^{-6} \text{ C}$ and (b), (d) $1.0 \times 10^{-4} \text{ C}$.

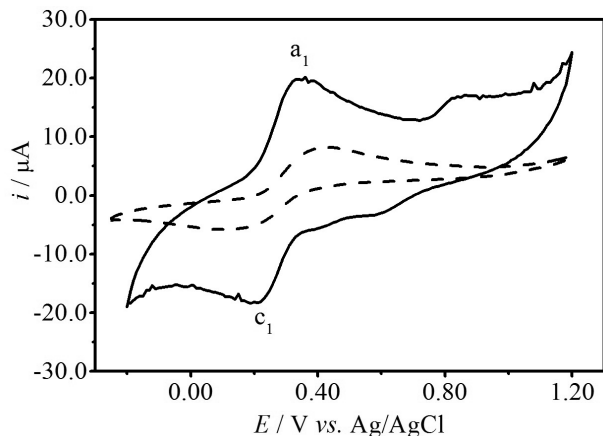


Figure 10. Typical voltammetric curves of the CPE, covered (solid curve) and not covered (dashed curve) by gold electrodeposits in $1.0 \times 10^{-3} \text{ mol L}^{-1} \text{ K}_4\text{Fe}(\text{CN})_6 + 0.10 \text{ mol L}^{-1} \text{ NaCl}$.

1.23 to 1.03) and increasing the anodic peak current (about 4.7 times higher).

Table 1 shows the 2^4 full factorial design and the voltammetric results for ΔE and i_{pa}/i_{pc} . It can be seen that the global average responses for ΔE (0.311 ± 0.344) and i_{pa}/i_{pc} (1.50 ± 0.95) showed higher standard deviations (with 95% of confidence in a normal distribution), which indicated that the electrodeposition conditions probably affected the CPE voltammetric response. Table 2 showed the main and interactions effects calculated and their percentage contribution, obtained by Pareto analysis,⁵⁶ which indicated that for i_{pa}/i_{pc} the main factors were 4 (24.5%), 14 (20.6%) and 234 (21.0%) interactions. In other hand, for ΔE the main factors were 3 (23.9%), 123 (11.548%) and 1234 (10.683%) interactions. It can be conclude that, in this electrochemical system studied, the deposition charge (factor 4) and deposition potential (factor 3) affected

Table 1. 2^4 full factorial design and the voltammetric results for ΔE and i_{pa}/i_{pc}

Experiment number	Factor				Response	
	1	2	3	4	$\Delta E / V$	i_{pa}/i_{pc}
1	-1	-1	-1	-1	0.310	1.92
2	+1	-1	-1	-1	0.470	2.24
3	-1	+1	-1	-1	0.380	2.05
4	+1	+1	-1	-1	0.550	1.35
5	-1	-1	+1	-1	0.230	1.36
6	+1	-1	+1	-1	0.060	0.97
7	-1	+1	+1	-1	0.270	2.40
8	+1	+1	+1	-1	0.120	1.59
9	-1	-1	-1	+1	0.250	0.95
10	+1	-1	-1	+1	0.240	1.25
11	-1	+1	-1	+1	0.530	1.09
12	+1	+1	-1	+1	0.480	1.30
13	-1	-1	+1	+1	0.530	1.09
14	+1	-1	+1	+1	0.100	2.11
15	-1	+1	+1	+1	0.070	1.03
16	+1	+1	+1	+1	0.390	1.34
Average response					0.311 ± 0.344	1.50 ± 0.95
Factor					Level	
					-1	+1
1	[HAuCl ₄] / (mol L ⁻¹)				1.0×10^{-6}	1.0×10^{-4}
2	[glycerol] / (mol L ⁻¹)				0	1.0×10^{-3}
3	deposition potential / V				+0.600	+0.200
4	deposition charge / C				1.0×10^{-6}	1.0×10^{-4}

the modified CPE performance as main factor, while the solution composition (HAuCl₄ and glycerol concentrations) affected only by interactions.

Moreover, it must be stressed that when employing a metallic electrodeposit as modifier, it is recommended to investigate how the chemical and electrochemical of metal

Table 2. Main and interactions effects and their percentage contribution obtained by Pareto analysis⁵⁶

Effect	$\Delta E / \text{mV}$	i_{pa}/i_{pc}	$\Delta E / \%$	$i_{pa}/i_{pc} / \%$
1	-0.008 ± 0.08	0.031 ± 0.2	0.054	0.107
2	0.085 ± 0.08	0.032 ± 0.2	6.274	0.116
3	-0.165 ± 0.08	-0.036 ± 0.2	23.938	0.147
4	0.012 ± 0.08	-0.464 ± 0.2	0.129	24.477
12	0.080 ± 0.08	-0.281 ± 0.2	5.602	8.977
13	-0.098 ± 0.08	0.000 ± 0.2	8.467	0.000
14	-0.011 ± 0.08	0.426 ± 0.2	0.103	20.615
23	-0.106 ± 0.08	0.178 ± 0.2	9.788	3.606
24	0.025 ± 0.08	-0.190 ± 0.2	0.548	4.112
34	0.089 ± 0.08	0.278 ± 0.2	6.938	8.753
123	0.115 ± 0.08	-0.002 ± 0.2	11.548	0.000
124	0.074 ± 0.08	0.078 ± 0.2	4.783	0.683
134	0.063 ± 0.08	0.204 ± 0.2	3.513	4.732
234	-0.093 ± 0.08	-0.430 ± 0.2	7.631	21.009
1234	0.110 ± 0.08	-0.153 ± 0.2	10.683	2.664

electrodeposition affect the electrochemical response of the interesting species, to identify if any electrodeposition parameters are main factor. In this case, a factorial planning is an important tool to find a good compromise in variable selection to obtain the metal electrodeposit and the modified CPE response to the specific analyte.

Conclusions

UV-Vis spectrophotometric analysis and voltammetric study indicated that AuCl_4^- was reduced to Au^0 since the initial potentials of reduction and, although glycerol did not complex Au^{3+} , glycerol affected the kinetic of electrodeposition. In addition, the Au electrodeposition was mixed controlled by mass transport and electron transfer, preceded by a chemical reaction, probably AuCl_4^- decomplexation. SEM images analysis showed that the gold electrodeposit covered totally some of the graphite flake by a homogeneous morphology, regardless of the HAuCl_4 concentration, deposition charge and glycerol added. Moreover, the modified CPE performance in a potassium ferrocyanide solution was influenced by the chemical and electrochemical parameters of electrodeposition. In this electrochemical system, deposition charge and potential were the main factors, while the solution composition (HAuCl_4 and glycerol concentrations) affected only by interactions with the other factors.

Acknowledgments

We would like to thank the Coordenação de Aperfeiçoamento de Pessoal de Nível Superior (CAPES) for their fellowships.

References

1. Svancara, I.; Vytras, K.; Kalcher, K.; Walcarius, A.; Wang, J.; *Electroanalysis* **2009**, *21*, 7.
2. Vytras, K.; Svancara, I.; Metelka, R.; *J. Serb. Chem. Soc.* **2009**, *74*, 1021.
3. Valery, H. G.; Ngono, T. R.; Saâdane, H.; Ennachte, M.; Khouilli, M.; Hafid, A.; Benoit, L.; Chtaini, A.; *Pharm. Anal. Acta* **2013**, *4*, 1.
4. Hu, C.; Wu, K.; Dai, X.; Hu, S.; *Talanta* **2003**, *60*, 17.
5. Bonifácio, V. G.; Junior, L. H.; Teixeira, M. F. S.; Fatibello-Filho, O.; *Microchem. J.* **2004**, *78*, 55.
6. Teixeira, M. F. S.; Ramos, L. A.; Filho, O. F.; Cavalheiro, E. T. G.; *Anal. Bioanal. Chem.* **2003**, *376*, 214.
7. Forzani, E. S.; Rivas, G. A.; Solis, V. M.; *J. Electroanal. Chem.* **1995**, *382*, 33.
8. Stoces, M.; Kalcher, K.; Svancara, I.; Vytras, K.; *Int. J. Electrochem. Sci.* **2011**, *6*, 1917.
9. Behpour, M.; Honarmand, E.; Ghoreishi, S. M.; *Bull. Korean Chem. Soc.* **2010**, *31*, 845.
10. Parvin, M. H.; Golivand, M. B.; Najafi, M.; Shariaty, S. M.; *J. Electroanal. Chem.* **2012**, *683*, 31.
11. Tashkhourian, J.; Nezhad, M. R. H.; Khodavesi, J.; Javadi, S.; *J. Electroanal. Chem.* **2009**, *633*, 85.
12. Atta, N. F.; Galal, A.; Azab, S. M.; *Analyst* **2011**, *136*, 4682.
13. Tsai, T. C.; Huang, F. H.; Chen, J. J. J.; *Sens. Actuators, B* **2013**, *181*, 179.
14. Arvand, M.; Dehsaraei, M.; *Mater. Sci. Eng., C* **2013**, *33*, 3474.
15. Gholivand, M. B.; Parvin, M. H.; *J. Electroanal. Chem.* **2011**, *660*, 163.
16. Wang, C. Y.; Hu, X. Y.; *Talanta* **2005**, *67*, 625.
17. Svancara, I.; Matousek, M.; Sikora, E.; Shachl, K.; Kalcher, K.; Vytras, K.; *Electroanalysis* **1997**, *9*, 827.
18. Atta, N. F.; Galal, A.; Abu-Attia, F. M.; Azab, S. M.; *J. Electrochem. Soc.* **2010**, *157*, F116.
19. Atta, N. F.; Galal, A.; Azab, S. M.; *Analyst* **2011**, *136*, 4682.
20. Atta, N. F.; Galal, A.; Azab, S. M.; *Int. J. Electrochem. Sci.* **2011**, *6*, 5066.
21. Afkhami, A.; Soltani-felehgari, F.; Madrakian, T.; *Talanta* **2014**, *128*, 203.
22. Dey, M. K.; Satpatti, A. K.; Sahoo, S.; Kameswaran, R.; Reddy, A. V. R.; Mukherjee, T.; *Anal. Methods* **2011**, *3*, 2540.
23. Luo, L.; Wang, X.; Ding, Y.; Li, Q.; Jia, J.; Deng, D.; *Anal. Methods* **2010**, *2*, 1095.
24. Shaidarova, L. G.; Chelnokova, I. A.; Gedmina, A. V.; Budnikov, G. K.; Ziganshina, S. A.; Mozhanova, A. A.; Bulkharaev, A. A.; *J. Anal. Chem.* **2006**, *61*, 375.
25. Safavi, A.; Maleki, N.; Tajabadi, F.; Farjami, E.; *Electrochem. Commun.* **2007**, *9*, 1963.
26. Safavi, A.; Maleki, N.; Farjami, F.; Farjami, E.; *J. Electroanal. Chem.* **2009**, *626*, 75.
27. Tesarova, E.; Baldrianova, L.; Hocevar, S. B.; Svancara, I.; Vytras, K.; Ogorev, B.; *Electrochim. Acta* **2009**, *54*, 1506.
28. Sopha, H.; Baldrianova, L.; Tesarova, E.; Hocevar, S. B.; Svancara, I.; Ogorev, B.; Vytras, K.; *Electrochim. Acta* **2010**, *55*, 7929.
29. Farahi, A.; Achak, M.; el Gaini, L.; el Mhammedi, M. A.; Bakasse, M.; *J. Food Drug Anal.* **2015**, *23*, 463.
30. Neto, B. B.; Scarmínio, I. S.; Bruns, R. E.; *Como Fazer Experimentos: Pesquisa e Desenvolvimento na Ciência e na Indústria*, 2ª ed.; Campinas Press: Campinas, Brasil, 2002.
31. Brenner, A.; *Electrodeposition of Alloys: Principles and Practice*, vol. I and II; Academic Press: New York, 1963.
32. Paunovic, M.; Schlesinger, M.; *Fundamentals of Electrochemical Deposition*; John Wiley & Sons: New York, 1998.
33. de Oliveira, G. M.; Silva, M. R.; Carlos, I. A.; *J. Mater. Sci.* **2007**, *42*, 10164.

34. de Oliveira, G. M.; Barbosa, L. L.; Broggi, R. L.; Carlos, I. A.; *J. Electroanal. Chem.* **2005**, *578*, 151.
35. Oliveira, E. M.; Finazzi, G. A.; Carlos, I. A.; *Surf. Coat. Technol.* **2006**, *200*, 5978.
36. Carlos, I. A.; Malaquias, M. A.; Oizumi, M. M.; Matsuo, T. T.; *J. Power Sources* **2001**, *92*, 56.
37. Fabio, G.; Carlos, I. A.; *Met. Finish.* **1997**, *95*, 70.
38. de Almeida, M. R. H.; Carlos, I. A.; Barbosa, L. L.; Carlos, R. M.; Lima-Neto, B. S.; Pallone, E. M. J. A.; *J. Appl. Electrochem.* **2002**, *32*, 763.
39. Pedroza, G. A. G.; de Souza, C. A. C.; Carlos, I. A.; de Andrade, L. R. P.; *Surf. Coat. Technol.* **2012**, *206*, 2927.
40. Miranda-Hernández, M.; Rincón, M. E.; *J. Solid State Electrochem.* **2005**, *9*, 646.
41. Curull, A.; Valentini, F.; Orlanducci, S.; Terranova, M. L.; *Indian J. Chem.* **2005**, *44A*, 956.
42. Zhu, L.; Tian, C.; Zhai, J.; Yang, R.; *Sens. Actuators, B* **2007**, *125*, 254.
43. Galandova, J.; Trnkova, L.; Mikelova, R.; Labudaa, J.; *Electroanalysis* **2009**, *21*, 563.
44. Kalachar, H. C. B.; Arthoba Naik, Y.; *Int. J. ChemTech Res.* **2011**, *3*, 1237.
45. Ramalakshmi, N.; Muthukumar, S.; Marichamy, B.; *Int. J. Chem. Phys. Sci.* **2013**, *2*, 16.
46. Arvand, M.; Dehsaraei, M.; *Mater. Sci. Eng., C* **2013**, *C33*, 3474.
47. Mazloun-Ardakani, M.; Rajabzadeh, N.; Benvidi, A.; Heidari, M. M.; *Anal. Biochem.* **2013**, *443*, 132.
48. Buoro, R. M.; Bacil, R. P.; da Silva, R. P.; da Silva, L. C. C.; Lima, A. W. O.; Cosentino, I. C.; Serrano, S. H. P.; *Electrochim. Acta* **2013**, *96*, 191.
49. Zaib, M.; Athar, M. M.; *Int. J. Electrochem. Sci.* **2015**, *10*, 6690.
50. Zhang, C.; Zhou, Y.; Tang, L.; Zeng, G.; Zhang, J.; Peng, B.; Xie, X.; Lai, C.; Long, B.; Zhu, J.; *Nanomaterials* **2016**, *6*, 7. DOI: 10.3390/nano6010007.
51. Bard, A. J.; Faulkner, L. R.; *Electrochemical Methods: Fundamentals and Applications*, 2nd ed.; John Wiley & Sons: New York, 2001.
52. Fletcher, S.; Halliday, C. S.; Gates, D.; Westcott, M.; Lwin, T.; Nelson, G.; *J. Electroanal. Chem. Interfacial Electrochem.* **1983**, *159*, 267.
53. Carretin, S.; McMorn, P.; Johnston, P.; Griffin, K.; Kiely, C. J.; Attard, G. A.; Hutchings, G. J.; *Top. Catal.* **2004**, *27*, 131.
54. Demirel, S.; Lehnert, K.; Lucas, M.; Claus, P.; *Appl. Catal., B* **2007**, *70*, 637.
55. Greef, R.; Peat, R.; Peter, L. M.; Pletcher, D.; Robinson, J.; *Instrumental Methods in Electrochemistry*; John Wiley: New York, 1985.
56. Zaviska, F.; Drogui, P.; Blais, J. F.; Mercier, G.; Lafrance, P.; *J. Hazard. Mater.* **2011**, *185*, 1499.

Submitted: March 22, 2016

Published online: May 9, 2016